

# Computing 3D Models of Rotating Objects from Moving Shading

Jiang Yu Zheng, Hiroshi Kakinoki, Kazuaki Tanaka and Norihiro Abe

Faculty of Computer Science and Systems Engineering  
Kyushu Institute of Technology  
Iizuka, Fukuoka 820, Japan

## Abstract

This work reconstructs 3D graphics model of an object from an image sequence taken during the object rotation. Shading and its motion information are used in estimating shapes of smooth surfaces between fixed edges from corners and patterns. Being different from conventional shape from shadings that use one or several images, we use an image sequence that provides not only shading but also its motion. Maximum diffused shading moving on surfaces is followed at each rotation plane and surface normals are obtained. Positions of points are estimated from moving shading using motion stereo principle. It is linear equations directly achieving the results rather than iterative computation in shape from shading using complex approximation.

## 1. Introduction

Recent progresses on multimedia, information network, and virtual reality provide a great opportunity for displaying 3D objects. Static and dynamic images have already been widely accessed through communication networks. New 3D model display tools such as VRML have also been developed for viewing objects through network. The objects can be commercial products, antiques and archaeological finds, folk arts and sculptures, etc.

How to input 3D models of objects conveniently and stably with low cost thus becomes a challenging problem. Although various laser range finders have been developed for input of 3D shape, they are still too expensive. We select video camera as the input device for 3D modeling. Our objective is as follows: getting a standard image sequence through network or recorded in video tape from users, we construct 3D models and return the data. To make reconstruction process robust, we fix the way of taking images, rather than just waving the camera in the space and solving a general problem. We rotate an object around an axis and take image sequences in the orthogonal direction. The rotation angle is controllable or measured in the images. We recover shape on each rotation plane using contours [1], highlights [2,3], edges [4,5], and shading according to their motions in the corresponding epipolar plane image. This paper introduces a new approach to get the model from shading motion.

Shape from shading algorithms have been extensively studied [6]. Although surface normal is easy to obtain using photometric stereo, acquiring shape itself is a difficult problem because of insufficient parameters. It was named as an "ill-posed problem" [9]. Regularization using iterative computation and approximation approaches have been developed [6,7,10].

With an image sequence of a rotating object, the problem of shape recovery becomes different. We give an approach that directly yields positions of surface points based on shading

motion; motion of gray level other than texture. Shading motion in the images represents motion of an oriented normal on the surface due to rotation. We pay more attention on shading motion than shading itself and focus on maximum diffused shading on each rotation plane. Our method deal with objects with both patterns and shading. We estimate surface reflectance, positions of surface points and connect the points into a graphics model. Shape is recovered directly without approximation and there is no accumulated error from propagation.

In the following, we will introduce our camera and light setting for observation, and compute positions of pattern edges and corners that segment an object into smooth surface regions of homogeneous reflectances. Then we estimate diffused surface reflectances of such regions. Based on the obtained information, surface points between fixed points are computed. This processes is carried out at each rotation plane using dynamically projected Epipolar Plane Image and the model is connected from shapes at all rotation planes.

## 2. Imaging Objects and Estimating Edges

### 2.1. Taking images of rotating objects

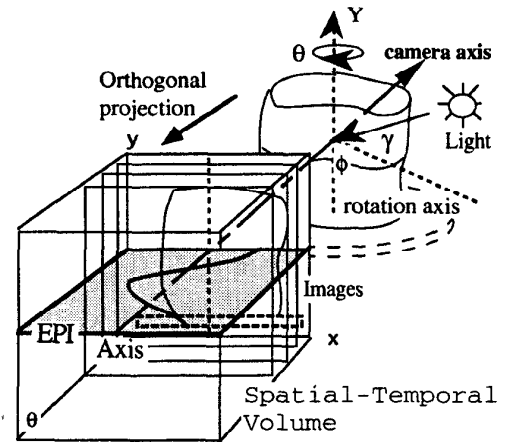
As an object rotates, a camera takes continuous images with its axis orthogonal to and passing the rotation axis as shown in Fig. 1. A point light is set at a known position. We assume orthogonal projection from scenes to the camera. Objects measured have only diffused reflection and have piece-wise constant reflectances. Gradation in which reflectance changes on a smooth surface is not allowed. For fixed points such as pattern edges and corners, we use shape from motion method to estimate their positions [4,5]. For surface between fixed points, we propose a new method named shape from moving shading.

For each rotation plane, we can determine an image line that is the image projection of the plane. An Epipolar-plane image is collected from the line. We put the camera centered coordinate system C-XYZ so that the x and y axes are aligned with EPI and the image of rotation axis, respectively. Fixed points thus have their trajectories in the EPIs as sinusoidal curves [5]. By tracking edges in EPI, we can compute positions of fixed points in the rotational planes. Figure 2 gives an example of EPI.

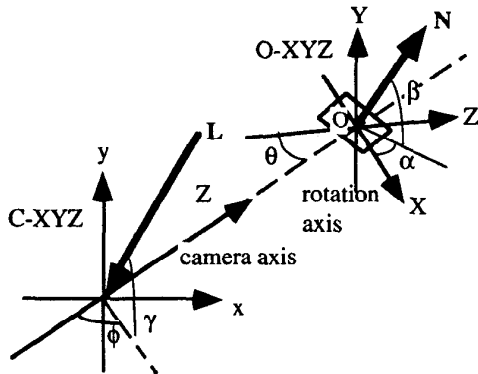
### 2.2 Estimating Edge Positions

A surface point  $P(X, Y, Z)$  described in the object centered coordinate system O-XYZ is continuously projected as  $p(x, y, \theta)$  in the spatial temporal volume during the rotation. The rotation angle  $\theta$  is known as clockwise in the analysis. The ray direction from a light is denoted by a vector  $L$  that has angle  $\gamma$  from the rotation plane and angle  $\phi$  from the camera direction in the rotation plane (Fig. 1(b)). The normal of the point is  $N(n_x, n_y, n_z)$  in the system O-XYZ. During the

rotation, the y component  $n_y$  along the rotation axis is constant and the component  $(n_x, n_z)$  in the rotation plane directs in turn to all orientations.



(a) Camera axis is set orthogonal to the rotation axis.



(b) Camera and object centered coordinates systems.

Fig. 1 Taking images of rotating objects and determining Epipolar Plane Images parallel to rotation the plane.

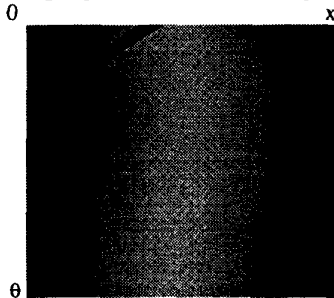


Fig. 2 An epipolar plane image shows moving shading at the rotation plane.

According to the camera geometry in Fig. 3, the viewing direction is  $V(-\sin\theta, 0, \cos\theta)$  in system O-XYZ. The image position of the point viewed at the rotation angle  $\theta$  can be written as

$$x(\theta) = P \cdot x = X(\theta) \cos\theta + Z(\theta) \sin\theta \quad (1)$$

where  $x$  is the unit vector of the horizontal image axis.

Tracking trajectory of a fixed point gives more than two

projections of the point and therefore the same number of the linear equations. We can use the least squared error method to compute 3D position of the point which is the crossing of multiple lines of sight determined by the projections (Fig. 3). The coordinates of P are

$$\begin{bmatrix} X \\ Z \end{bmatrix} = \frac{1}{\sum_{\theta=\theta_1}^{\theta_n} \sin^2 \theta \sum_{\theta=\theta_1}^{\theta_n} \cos^2 \theta - \left( \sum_{\theta=\theta_1}^{\theta_n} \cos \theta \sin \theta \right)^2} \times \begin{bmatrix} \sum_{\theta=\theta_1}^{\theta_n} x(\theta) \cos \theta \sum_{\theta=\theta_1}^{\theta_n} \sin^2 \theta - \sum_{\theta=\theta_1}^{\theta_n} x(\theta) \sin \theta \sum_{\theta=\theta_1}^{\theta_n} \sin \theta \cos \theta \\ \sum_{\theta=\theta_1}^{\theta_n} x(\theta) \sin \theta \sum_{\theta=\theta_1}^{\theta_n} \cos^2 \theta - \sum_{\theta=\theta_1}^{\theta_n} x(\theta) \cos \theta \sum_{\theta=\theta_1}^{\theta_n} \cos \theta \sin \theta \end{bmatrix} \quad (2)$$

where  $x(\theta)$  is the x coordinate of a trace at rotation angle  $\theta$ , located by filtering EPI with an edge detector.

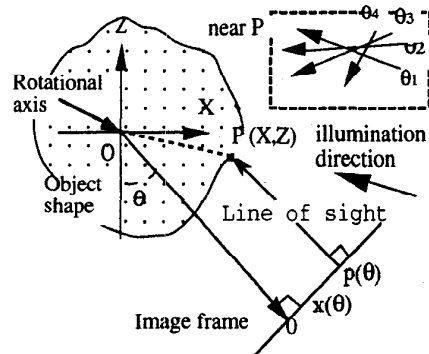


Fig. 3 Camera and object relation in a rotation plane.

### 3. Estimation of Diffused Reflectance

If there are only sparse fixed points on object, model construction has to rely on other visual cues. We try to use shading in this work. From the EPI in Fig. 2, we can clearly perceive 3D shape conveyed by shading which comes out from swiveling real shape at the rotation plane. We will explore the way to extract real shape from the changing shading. Before that, we show a surface point change in shading is a sinusoidal function. That means, for a known point, the intensity along its sinusoidal trajectory is also a sinusoidal function of the rotation angle. This allows us to estimate surface reflectances for further computation of surface points.

If an object has only diffused reflection, we have the typical equation

$$I = RL \cos \langle N, L \rangle \quad (3)$$

describing shading at a point, where  $I$  is image intensity,  $R$  is diffused reflectance and  $L$  is irradiance of light. If we denote surface normal at the point as  $N = (\cos\beta \cos\alpha, \sin\beta, \cos\beta \sin\alpha)$  in the system O-XYZ attached to the object and  $\beta, \alpha$  are Euler angles, it becomes  $N(\theta) = (\cos\beta \cos(\alpha - \theta), \sin\beta, \cos\beta \sin(\alpha - \theta))$  in the system C-XYZ after rotating  $\theta$  degree. The ray is  $L(\cos\gamma \cos(\phi - \pi/2), \sin\gamma, \cos\gamma \sin(\phi - \pi/2))$  in the system C-XYZ. The image intensity of the point viewed at angle  $\theta$  becomes

$$I(\theta) = RL (\cos\beta \cos(\alpha - \theta), \sin\beta, \cos\beta \sin(\alpha - \theta)) \cdot$$

$$\begin{aligned}
& (\cos\gamma\cos(\phi-\pi/2), \sin\gamma, \cos\gamma\sin(\phi-\pi/2)) \\
& = RL\cos\beta\cos\gamma\sin(\theta-\alpha+\phi) + RL\sin\beta\sin\gamma \\
& = A\sin(\theta-\Lambda) + B
\end{aligned} \tag{4}$$

$$\begin{aligned}
\text{where } A &= RL\cos\beta\cos\gamma > 0, & \beta, \gamma &\in (-\pi/2, \pi/2) \\
B &= RL\sin\beta\sin\gamma,
\end{aligned}$$

$$\Lambda = \alpha - \phi \tag{5}$$

The change of shading turns out to be a sinusoidal function of  $\theta$ , since terms A and B are constant during the rotation for the point. It is also obvious that the point gets the maximum shading when its xz component of normal rotates to the light orientation in the rotation plane. This can be verified in Eq. 4. When the normal orientation  $\alpha - \theta$  is towards the light direction  $\phi - \pi/2$  in the system C-XYZ, we have

$$\sin(\theta - \Lambda) = \sin(\theta - \alpha + \phi) = 1$$

so that  $I(\theta)$  reaches the maximum.

Based on the above discussion, the relative diffused reflectance of each region is measured at a point next to a fixed point. If we detect a trajectory of edge from either a pattern or a corner, we can obtain a series of image points  $p(x_i, \theta_i)$  next to the trajectory (in a few pixels wide). These image points with intensities  $I_i$  are considered as a moving trajectory of a surface point in the vicinity. Because  $\alpha, \beta$  are constant for the point and light direction  $\phi, \gamma$  are constant for all points, terms A and B are constant for the near-edge point (denoted by  $A_e$  and  $B_e$ ) and equation 4 is linear for term  $\sin(\theta - \Lambda)$ . We can use the least squared error method to obtain the unknowns  $A_e$  and  $B_e$ . Figure 4 gives an example where a sinusoidal function is fitted to intensities collected from points next to an edge trace in EPI.

Because angle  $\gamma$  is known from the light setting, RL can be computed from two terms  $A_e$  and  $B_e$  as

$$RL = ((A_e/\cos\gamma)^2 + (B_e/\sin\gamma)^2)^{1/2} \tag{6}$$

for a non-zero  $\gamma$ , which gives the relative reflectance of the surface region. The normal of the focused point is

$$\beta_e = \arcsin(B_e / RL\sin\gamma) \tag{7}$$

For a trajectory of edge, this process is done on its two sides to yield relative reflectances of its two neighbor regions.

If there is no edge in an EPI, which means a surface is completely smooth at the rotation plane, we can use reflectance from another EPI at the nearest height. If there is no edge in any EPI, which means the object is smooth everywhere and has a uniformed reflectance, we need to know a 3D point to do the reflectance estimation as above. The 3D position of the point could be from contour [1,10].

## 4 Shape and Normal Estimations

### 4.1. Normal Estimation from Maximum Shading

Now we can discuss how to analyze EPIs for constructing shapes on parallel rotation planes. After finding corners and pattern edges, the remaining regions are smooth surfaces with constant reflectances. In a region of EPI segmented by trajectories of fixed points, we can find a trace of pixels with the brightest intensities. Such a trace in Fig. 2 can be noticed almost at the center of the EPI. It passes all trajectories of surface points in that region and is in fact a connection of all maximum intensity positions on the trajectories, although those trajectories of surface points themselves are unable to be distinguished in the EPI. On such a bright trace, the xz

components of surface normals face to the light orientation in the rotation plane. We name the trace as *maximum diffused trace*.

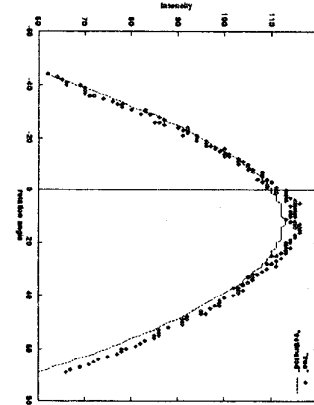


Fig. 4 Estimating relative reflectance of a surface region from intensity changes of a known point. The horizontal axis is intensity and the vertical axis is the rotation angle. Dots in the figure are measured data along a trajectory of edge and a sinusoidal curve is fitted.

Using intensities on the maximum diffused trace, we will figure out surface normals of surface points. Supposing a point  $p(\theta, x(\theta))$  on the trace is located, the intensity there becomes

$$I_{\max}(p) = A_p + B_p = RL\cos(\beta - \gamma) \tag{8}$$

$$\text{at } \theta - \Lambda_p = \pi/2 \tag{9}$$

according to Eqs. 4, 5. The maximum intensity hence depends on the y component of surface normal, which can be computed by

$$\beta_p = \pm \arccos(I_{\max}(p) / RL) + \gamma \tag{10}$$

$$\text{and } \alpha_p = \phi + \theta - \pi/2 \tag{11}$$

At this point, we obtained surface normal of a point up to two possible solutions. Only one of them is true. Based on Eq. 5,  $A_p$  and  $B_p$  have also two corresponding solutions for the point.

### 4.2. Computing Positions of Surface Points

In order to estimate shape, we use a strategy of hypothesis and verification. We assume both solutions of the normal in Eq. 10 are correct and use them to determine the 3D positions of the surface point. Because shading of a surface point changes as a sinusoidal function along its sinusoidal trajectory in the EPI, we can use this rule to test the obtained positions so as to choose one whose changing intensities better agrees with the sinusoidal function

Let us see how a position can be computed using one normal. If a point on the maximum diffused trace is located at  $\theta$ , we investigate two projections of the same surface point that have angle difference  $\Delta\theta$  from  $\theta$ . Based on the result given by Eq. 4, they should have intensities

$$\begin{aligned}
I_1(\theta + \Delta\theta) &= A_p \sin(\theta + \Delta\theta - \Lambda(\theta)) + B_p \\
I_2(\theta - \Delta\theta) &= A_p \sin(\theta - \Delta\theta - \Lambda(\theta)) + B_p
\end{aligned} \tag{12}$$

if a normal or  $A_p$  and  $B_p$  are given. Along angles  $\theta + \Delta\theta$  and  $\theta - \Delta\theta$  in the EPI, we search two positions  $x_1(\theta + \Delta\theta)$  and  $x_2(\theta - \Delta\theta)$  that have intensities  $I_1(\theta + \Delta\theta)$  and  $I_2(\theta - \Delta\theta)$  respectively. This process is shown in Fig. 5. The two located positions can

determine the sinusoidal trajectory of the surface point. Searching the projections are similar as matching correspondences in motion stereo. The difference is that the projections here are not matched by edge attributes, but are determined according to their shadings.

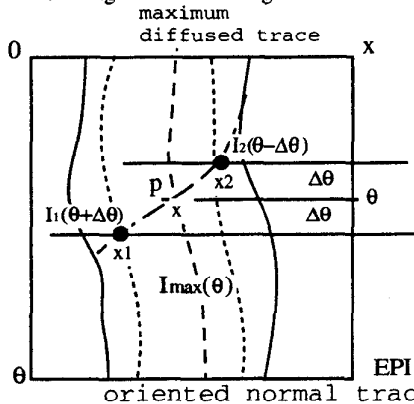


Fig. 5 Searching two projections of a surface point according to estimated shadings.

Next step is to compute shape directly instead of netting the shape with computed normals. According to Eq. 1, the lines of sight passing the projections of the surface point are

$$\begin{aligned} x_1(\theta+\Delta\theta) &= X(P) \cos(\theta+\Delta\theta) + Z(P) \sin(\theta+\Delta\theta) \\ x_2(\theta-\Delta\theta) &= X(P) \cos(\theta-\Delta\theta) + Z(P) \sin(\theta-\Delta\theta) \end{aligned} \quad (13)$$

We can compute the position of the surface point by

$$\begin{pmatrix} X \\ Z \end{pmatrix} = \frac{1}{\sin 2\Delta\theta} \begin{pmatrix} -\sin(\theta-\Delta\theta) & \sin(\theta+\Delta\theta) \\ \cos(\theta-\Delta\theta) & -\cos(\theta+\Delta\theta) \end{pmatrix} \begin{pmatrix} x_1(\theta+\Delta\theta) \\ x_2(\theta-\Delta\theta) \end{pmatrix} \quad (14)$$

It is a motion stereo method that gives the surface point from crossing of two lines of sight.

To verify the correctness of the hypothesized normals and their corresponding positions, we generate two sinusoidal traces from the two solutions using Eq. 13 and pick up pixels on the traces to compare their values with the sinusoidal intensity functions described by Eq. 4. We choose one normal and the position that has high value fitting the criterion.

## 5. Model Recovery from Moving Shading

The maximum shading moves on surface during rotation and surface points in turn face the light. Similarly, other values of shading also shift on surface. Although, in a rotation plane, the  $y$  components of surface normals are not guaranteed to be constant for all points, it will change smoothly between two fixed points. Otherwise, there should appear a corner that is a fixed point. The positions with intensities  $I(\theta+\Delta\theta)$  computed from corresponding maximum diffused trace also form a continuous trace in the EPI. We call such a trace *oriented normal trace*, since for all points on such a trace, their surface normals keep the same angle  $\Delta\theta$  from the ray in the rotation plane. The oriented normal trace displays motion of shading or motion of an oriented normal on the surface.

We use moving shading to figure out shape of the object at the rotation plane. As we track the maximum diffused trace in an EPI, we compute surface normals and matching two projections. The correspondences obtained on two oriented normal traces are used in estimating positions of surface points and connected into boundary at the rotation plane.

The types of maximum diffuse traces are qualitatively related to curvature signs of the shape on the rotation plane which is convex, planer, or concave. This is similar to what has been explored in highlights [2]. After shape on each rotation plane is established, we connect them together to produce a graphics model.

Although a maximum diffused trace is easy to be detected in an EPI, the locations of its points are not accurate because they are found at the peaks of sinusoidal functions. The location of an oriented normal trace is relatively accurate. This is the reason we do not use the maximum diffused trace directly but oriented normal traces in our shape estimation. The inaccuracy of the maximum diffused trace will not influence the accuracy of oriented normal traces since only intensity other than position of the maximum diffused trace are used in locating oriented normal traces.

## 6. Experiments

We have done experiments on real objects. To test how correct the produced shapes are, we select objects with less pattern and texture. More textures and corners will certainly improve the results, since an edge has more than two projections visible during the rotation and the least squared error method provides high accuracy. Figure 6 displays two objects for modeling. They are put on a computer controlled turn table [1]. We attach a dark line to object to yield edges on the surface. The light is above the camera so that  $\phi=0$ . This makes the maximum diffused trace equally divide EPI region of object for finding oriented normal traces.

For each object, an EPI is displayed with extracted the maximum diffused trace and two oriented normal traces (Fig. 7). Although the locations of the maximum diffused points are not accurate enough to form a trace for increasing  $\theta$ , precise localization of the oriented normal traces is not influenced. Object shapes on the rotation plane are displayed in Fig. 8. We can see the circular shape is recovered well for the pottery. The recovered shape of the bottle in the rotation plane is overlapped with its true shape which is extracted from an image taken from the top. The maximum relative shape error for the bottle is 4%. The shapes at all rotation planes are then connected into 3D models shown in Fig. 9.

Because the computation of shape is applied locally, position error will not propagate to other parts. The position error of this method is mainly from the existence of specular reflectance on objects that influences the fitting of surface reflectance function and tracking of maximum diffused traces. The resulted accuracy of the shape depends on object size and is possible to be measured relatively.

The limitation of this method is probably on complicated objects such as deep waving shapes, which yield complex types of traces. The image resolution for tracking traces must be considered.

## 7. Conclusion

In this paper, we proposed an algorithm to obtain 3D models of objects by rotating them. Shading moving on an EPI is followed for detecting an oriented normal moving on surfaces. Shape is computed by linear equations as motion stereo. Relative reflectance on diffused surface regions and surface normals can also be computed. The method is simple and easy to be realized with robustness. We will further work on complicated objects to test the algorithm.

**References**

[1] J.Y. Zheng, "Acquiring 3D models from sequences of contours", IEEE PAMI, Vol.16, No.2, Feb. pp.163-178, 1994.  
 [2] J. Y. Zheng, Y. Fukagawa, T. Ohtsuka, N. Abe, "Acquiring 3D models from rotation and a highlight", 12th ICPR, Vol. 1, pp. 331-336, 1994.  
 [3] J. Y. Zheng, Y. Fukagawa, N. Abe, Shape and Model from Specular Motion, 5th ICCV, pp.92-97, 1995.  
 [4] J. Y. Zheng, and F. Kishino, "Verifying and combining different visual cues into a complete 3D model", CVPR92, pp. 777-780, 1992.  
 [5] J. Y. Zheng, H. Kakinoki, K. Tanaka, and N. Abe, "Acquiring 3D models from fixed point during rotation", 3th ICARCV, Vol. 1, pp.459-463, 1994.  
 [6] K. P. Horn and M. J. Brooks, "Shape from shading", MIT Press, Cambridge, MA, 1989.  
 [7] A. Pentland, "Local shading analysis", IEEE PAMI, 6:170-187, 1984.

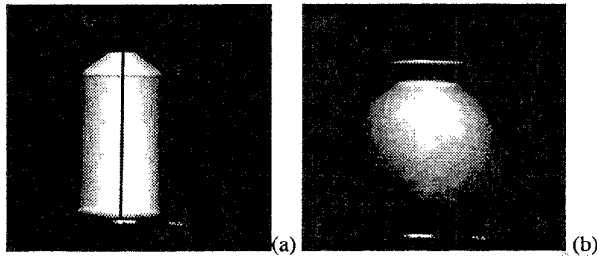


Fig. 6 Objects for modeling.(a) a plastic bottle. (b)pottery.

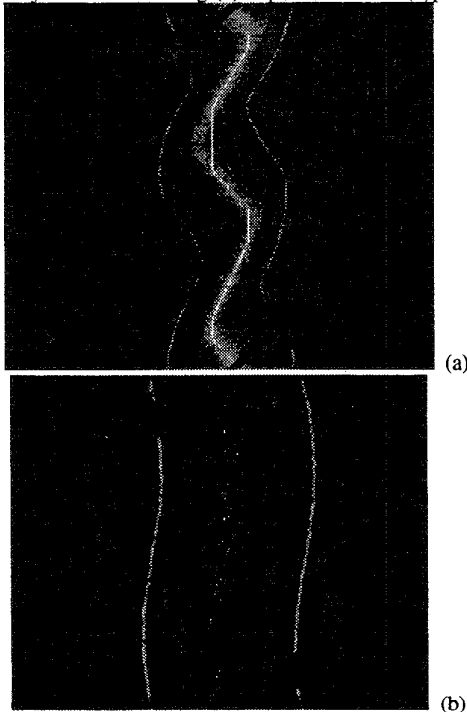


Fig. 7 Epipolar-plane images of two objects with extracted maximum diffused trace and oriented normal traces. (a) an EPI of bottle with maximum diffused trace and oriented normal

traces. (b) an EPI of the pottery.

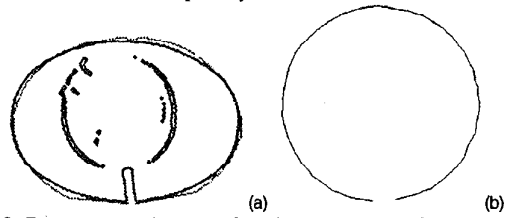


Fig. 8 Recovered shapes of objects in Fig. 7 on rotation planes. (a) Shape of the bottle at a rotation plane. The gray curve is the recovered shape and the dark curves are true shape. (b) shape of the pottery at a rotation plane.

[8] R. J. Woodham, "Gradient and curvature from photometric stereo including local confidence estimation", J. Opt. Soc. Amer., Vol. 11, no. 11, 3050-3068, 1994.  
 [9] J. Aloimonos and A. Bandyopadhyay, "Active vision", 1st ICCV, pp.35-55, 1987.  
 [10] J. Lu and J. Little, "Reflectance function estimation and shape recovery from image sequence of a rotating object", 5th ICCV, pp. 80-86, 1995.  
 [11] R. Vaillant and O. D. Faugeras, "Using extremal boundaries for 3D object modeling", IEEE PAMI, Vol. 14, No. 2, pp. 157-173. Feb. 1992.  
 [12] H. Baker, and R. Bolles, "Generalizing epipolar-plane image analysis on the spatiotemporal surface", CVPR-88, pp.2-9, 1988.

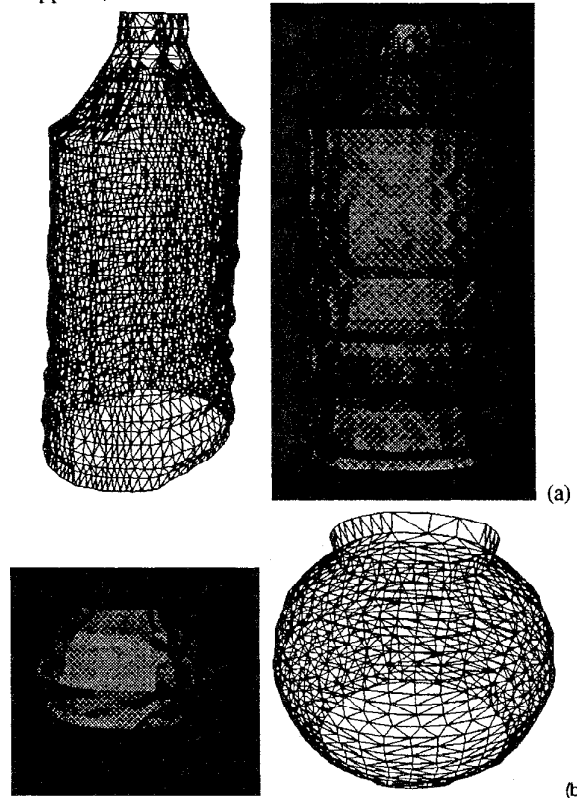


Fig. 9 Reconstructed models of objects in Fig. 6 connected by triangular patches and displayed in shading mode by computer graphics. (a) bottle.(b) pottery.